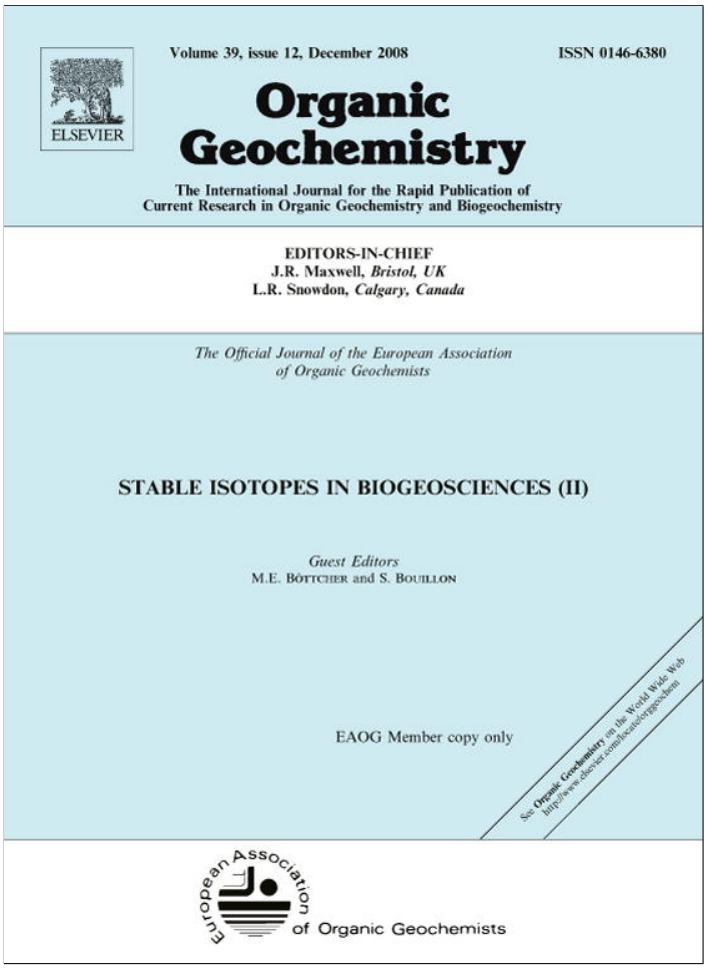

Organic Geochemistry 39 (2008) 1800–1815

Contents lists available at ScienceDirect

Organic Geochemistry

journal homepage: www.elsevier.com/locate/orggeochem

Comparison of phenyldibenzothiophene distributions predicted from molecular modelling with relevant experimental and geological data

M.J. Rospondek [a,*], M. Szczerba [a,b,c], K. Malek [c], M. Góra [c], L. Marynowski [d]

[a] Institute of Geological Sciences, Jagiellonian University, ul. Oleandry 2A, 30-063 Kraków, Poland
[b] Institute of Geological Sciences, Polish Academy of Sciences, ul. Senacka 1, 30-063 Kraków, Poland
[c] Faculty of Chemistry, Jagiellonian University, ul. Ingardena 3, 30-063 Kraków, Poland
[d] Faculty of Earth Sciences, Silesian University, ul. Będzińska 60, 41-200 Sosnowiec, Poland

ARTICLE INFO

Article history:
Received 26 February 2008
Received in revised form 14 June 2008
Accepted 30 June 2008
Available online 14 August 2008

ABSTRACT

Evaluation of the relative thermodynamic stabilities of phenyldibenzothiophenes, by means of molecular modelling, has led to the prediction of their equilibrium mixture composition. The calculated equilibrium composition shifts towards that obtained in a laboratory maturation experiment and encountered in mature geological samples (mean vitrinite reflectance $R_r \gtrsim 1.2\%$). Close inspection of a suite of samples, having in common hydrothermal oxidation of organic matter, but varying in maturity, suggests that phenyldibenzothiophenes can isomerise and also cyclise to triphenyleno[1,12-*bcd*]thiophene. Both reactions are thermodynamically possible as a result of the relative decrease in enthalpy along the reaction paths and the resulting competition for the precursor 1-phenyldibenzothiophene. Changes in the phenyldibenzothiophene positional isomer distributions from kinetically to thermodynamically controlled mixtures are likely to be achieved with an acid catalysed 1,2-phenyl shift, as suggested from our maturation experiment. To validate this hypothesis, *ab initio* quantum chemical calculations (DFT) were performed, leading to the localisation of potential transition states as well as the determination of activation energies in gas phase and aqueous solution. The isomerisation barriers are significantly lowered by acid catalysis. They are in the range from $\Delta E_{(aq)}$ 20.5 to 28.7 kcal/mol, consistent with the early beginning of the isomerisation observed for our samples. With increasing maturity, 1-PhDBT decays rapidly. At very advanced maturity stages the process is often accompanied by the appearance of triphenyleno[1,12-*bcd*]thiophene, suggesting its simultaneous formation by cyclisation/oxidation. The oxidation is most likely associated in nature via thermochemical sulfate reduction (TSR). The modelling of such a reaction with thiosulfates yielded an energy barrier $\Delta E_{(aq)}$ of ca. 64.7 kcal/mol, only when the initial step involved protonation. This energy seems relevant to very advanced stages of diagenesis/catagenesis. The modelled barrier can be lowered by 2–3 kcal/mol at significantly elevated fluid temperatures as a result of changes in the physical properties of water.

1. Introduction

The distribution of polycyclic aromatic compounds (PACs) can provide valuable information on the origin (e.g. Strachan et al., 1988; Killops and Massoud, 1992; Otto and Simoneit, 1999), diagenesis (e.g. Püttmann and Villar, 1987; Püttmann et al., 1990; Marynowski et al., 2002; Rospondek et al., 2007) and burial history of sediments and sedimentary rocks enriched in organic matter (e.g. Radke et al., 1982, 1986, 2000) as well as petroleum (e.g. Chakhmakhchev et al., 1997). In samples of low maturity, the PAC distribution is usually kinetically (origin) controlled, though it can be also thermodynamically controlled at more advanced stages of maturity, depending on the specific PAC stability (e.g. van Duin et al., 1997). To make

* Corresponding author. Tel.: +48 126632657; fax: +48 126632270.
E-mail address: m.rospondek@uj.edu.pl (M.J. Rospondek).

0146-6380/$ - see front matter © 2008 Elsevier Ltd. All rights reserved.
doi:10.1016/j.orggeochem.2008.06.012

a distinction between both of these idealised end member distributions, molecular modelling can be applied. Its application with a view to understanding the distributions of many PACs of geochemical relevance has proven to be useful (e.g. Budzinski et al., 1993; Oldenburg et al., 2002). For mature samples the modelled thermodynamic equilibrium composition has been used to define the final isomer distribution of alkylated PACs (e.g. Budzinski et al., 1993; van Duin et al., 1997). However, molecular modelling has not been used to disclose the natural distribution of polyaromatic thiophene derivatives, which are commonly used as maturity indicators, e.g. alkyl dibenzothiophenes (Radke and Willsch, 1994; Radke et al., 1986; Chakhmakhchev et al., 1997). A number of molecular maturity parameters (Radke et al., 1982, 2000), like the methyldibenzothiophene ratio (MDR; Radke et al., 1986; Radke and Willsch, 1994), are based on variation in the relative stability of PAC positional isomers. Changes in the relative abundances of methyldibenzothiophene isomers (for numbering system see Appendix A) have been attributed to the difference in generation yield profiles and isomerisation reactions with increasing thermal stress on burial (Radke et al., 1986, 2000; Radke and Willsch, 1994). Preliminary studies have shown that alkyl dibenzothiophenes react differently from phenyldibenzothiophenes (PhDBTs) to increasing maturity. In this study, phenyldibenzothiophene isomerisation is explored and compared with that of methyldibenzothiophene. The composition at thermodynamic equilibrium is modelled and compared with the compound distributions in mature geological samples, such as hydrothermal petroleum from the Guyamas Basin, California. To gain a better insight into the conditions of phenyldibenzothiophene positional isomer formation in nature, a laboratory maturation experiment, based on clay catalysed isomerisation, was performed, suggesting that a 1,2-phenyl shift may be one of the important mechanisms influencing the natural distributions (Rospondek et al., 2007). To validate the hypothesis, quantum chemical calculations were also carried out in order to localise the potential transition states and to determine the activation energy. Furthermore, the identification of triphenyleno[1,12-*bcd*]thiophene (TPT), both in rock samples as well as in maturation experiment products, indicates that phenyldibenzothiophene cyclises, a hypothesis that was tested by modelling the reaction kinetics.

2. Samples and methods

2.1. Samples

All samples from our database containing phenyldibenzothiophenes were selected (Table 1). The samples represent marine rocks containing mostly Type II kerogen (Rospondek et al., 1993; Kotarba et al., 2006), except for the samples from the Carpathians (Rospondek and Marynowski, 2004; Środoń et al., 2006) and the base of the Zechstein sections (Sun et al., 1995), which contain admixtures of Type III. Their diagenesis/catagenesis was influenced by oxidising hydrothermal solutions (Marynowski et al., 2002; Rospondek et al., 2007). The circulation of hot aqueous fluids along sedimentary, lithology or tectonic boundaries resulted in the formation of significant gradients in pH and redox conditions, as well as increased concentrations of transition metals and sulfur species during rock diagenesis/catagenesis. Such events are recorded in rocks as hematite/goethite pseudomorphs after sedimentary often framboidal pyrite, occurring close to transition metal sulfides (e.g. Oszczepalski, 1989). The samples were collected from the following localities:

1. Middle and Upper Devonian carbonates and shales from the Holy Cross Mountains, South Poland. These are represented by a series of samples from Kowala, Góra Łgawa, Radkowice, Piskrzyn and Laskowa Góra having R_r from ca. 0.5% to 1.2% (Marynowski et al., 2000, 2002). In this region, the Upper Devonian rocks host hydrothermal reddish thick calcite veins and a copper, zinc and lead sulfide mineralisation (e.g. Miedzianka, Miedziana Góra).
2. Equivalent to the Holy Cross Mountains rocks from the Kraków-Silesia Monocline, Dębnik Anticline. The maturity (R_r > ca. 1.4%) is due to the thermal/hydrothermal influence of the large Upper Carboniferous/Permian (Nawrocki et al., 2007) rhyodacite intrusion (Lewandowska, 1991, 2000).
3. Upper Permian (Zechstein) limestones, dolomites, marls and shales (Kupferschiefer) from the Fore-Sudetic Monocline and North Sudetic Trough, SW Poland (Oszczepalski, 1989; Rospondek et al., 1994; Bechtel et al., 2001). The samples were collected from the Polkowice-Sieroszowice and Rudna mines in the areas where a hematite stained irregular hydrothermal oxidation front "Rote Fäule", arising from underlying strata, penetrates the organic-rich marine sedimentary sequence. Interestingly, the samples from the Lubin mine lack the compounds of interest – presumably, because of the absence of the oxidising zones. The maturity is from ca. R_r 0.6% to 0.7%.
4. The Western Carpathians, Southern Poland Cretaceous and Tertiary Flysch shales with maturity in the range R_r 0.9–1.5%, originating from the Podhale Trough (see Rospondek and Marynowski, 2004; Środoń et al., 2006).
5. Hydrothermal petroleum from the Guaymas Basin, Gulf of California, Mexico. This is generated in active, sediment-covered hydrothermal systems of the oceanic rift zone in the tectonic graben basin, which is filled with thick diatomaceous oozes and terrigenous silty muds (see, e.g. Kawka and Simoneit, 1990). The conversion of semi-recent kerogen into petroleum occurs in high-temperature water ca. 300 °C and at least 200 bar (Simoneit, 1993).

2.2. Vitrinite reflectance

Vitrinite reflectance (R_r) analysis was carried out using an AXIOPLAN II Microscope, adapted for reflected white light observation, in oil immersion and a total magnification of 500×. The reflectance standard used has R_r 0.62%. About 100 vitrinite grains were measured for each sample.

Table 1
Sample description, bulk data and relative concentration (wt%) of phenyldibenzothiophene isomers

Locality	Lithology (age)	R_r (%)	TOC (%)	EOM (mg/g TOC)	Phenyldibenzothiophenes (wt%)			
					1-	4-	2-	3-
Holy Cross Mountains, Poland (Devonian)								
Bukowa Góra	Shale (Emsian)	1.15	n.d.[a]	n.d.	0.0	37.7	39.2	23.1
Kowala-1 (851 m)	Dolostone (Eifelian)	0.64	n.d.	n.d.	25.2	27.7	29.8	17.2
Piskrzyn	Dolostone (Eifelian)	0.73	n.d.	n.d.	11.8	28.7	34.5	25.0
Piskrzyn	Shale (Eifelian)	0.76	n.d.	n.d.	32.8	30.6	24.1	12.5
Radkowice	Greenish shale (Eifelian)	0.65	1.13	10	31.7	34.1	19.8	14.4
Radkowice	Greenish dolostone (Eifelian)	0.62	0.80	12	23.8	38.1	20.7	17.3
Laskowa Góra	Dolostone (Eifelian?)	1.20	0.37	11	1.7	26.3	37.4	34.6
Laskowa Góra	Greenish shale (Eifelian?/Givetian?)	1.15	n.d.	n.d.	0.3	27.3	47.8	24.6
Janczyce-1 (943 m)	Dolostone (Givetian?)	n.f.	0.03	20	9.3	26.6	40.9	23.2
Jaworznia	Limestone (Frasnian)	0.63	0.01	20	13.6	41.5	25.4	19.5
Sitkówa-Kowala	Limestone (Givetian)	0.63	0.25	68	29.2	27.4	23.8	19.7
Kowala K1	Black shale (Frasnian)	0.57	3.68	18	29.9	31.3	22.6	16.2
Kowala K2	Black shale (Frasnian)	0.54	8.17	15	28.5	30.9	24.3	16.3
Kowala K3	Black shale (Frasnian)	0.55	4.00	30	31.8	32.4	20.3	15.4
Kowala K4	Black shale (Frasnian)	0.55	0.89	69	34.2	30.9	19.2	15.6
Kowala K5	Black shale (Frasnian)	0.57	4.14	43	37.8	29.5	16.3	16.4
Panek (by Bolechowice)	Limestone (Frasnian)	0.66	0.14	21	27.2	35.9	21.3	15.6
Góra Łgawa	Marly limestone (Famennian)	0.52	0.73	27	40.9	31.2	14.9	13.0
Kraków-Silesian Monocline, Dębnik Antycline, Southern Poland (Devonian)								
Dębnik	Limestone (Givetian)	n.f.[b]	n.d.	n.d.	17.0	27.9	28.3	26.7
Dębnik	Marly shale (Frasnian)	1.4	1.45	13	0.0	31.6	36.9	31.6
Fore-Sudetic Monocline. South-Western Poland (Zechstein)								
Lubin LE-I/0	"Basal" dolostone	n.f.	0.4	4	26.9	25.3	28.3	19.6
Polkowice PW-II/1	Laminated reddish dolostone	n.f.	1.00	6	21.0	33.1	24.6	21.3
Polkowice PW-III/1	Reddish/black marly shale (spots of hematite)	n.f.	n.d.	n.d.	15.6	41.5	28.1	14.7
Polkowice PW-III/2	Reddish limestone (spots of hematite)	0.68	n.d.	n.d.	20.9	34.5	26.3	18.3
Sieroszowice S1	Reddish/black shale (spots of hematite)	0.72	6.1	4	37.4	24.1	21.4	17.2
Sieroszowice S3	Reddish limestone (with spots of hematite)	n.f.	0.7	6	30.9	28.7	22.7	17.7
Rudna	Bitumen cementing sandstone	n.f.	n.d.	n.d.	33.6	25.2	23.9	17.3
North-Sudetic Trough, South-Western Poland (Zechstein)								
Konrad Cu	Marly limestone	n.f.	n.d.	n.d.	52.8	26.9	12.6	7.7
Konrad Pb	Marly limestone	0.68	n.d.	n.d.	51.4	32.1	10.1	6.4
Konrad "Rote Fäule"	Reddish/black marly shale(spots of hematite)	0.70	n.d.	n.d.	28.0	33.6	21.7	16.8
Podhale Trough, the Carpathians, Southern Poland								
Zakopane	Flysch shale (Paleogene)	0.9	n.d.	n.d.	15.8	34.2	23.6	26.4
Poronin PAN-1 borehole (depth 1912 m)	Flysch shale (Cretaceous)	1.5	0.12	n.d.	0.0	45.3	33.8	20.9
Gulf of California, Mexico								
Guaymas Basin	Hydrothermal oil		n.d.	n.d.	0.0	24.8	30.3	45.0
Laboratory maturation experiment (see: Paragraph 2.5.)								
PhDBT isomer mixture					2.9	16.9	38.7	41.7

[a] Not detected (n.d.).
[b] Not found (n.f.).

2.3. Gas chromatography–mass spectrometry

Component identification was achieved by means of gas chromatography–mass spectrometry (GC–MS) as described elsewhere (e.g. Rospondek et al., 2007).

2.4. Standard compounds

Identification of phenyldibenzothiophenes was achieved using chromatographic and spectral comparison with 1-, 2-, 3- and 4-phenyldibenzothiophenes (Chiron, Trondheim, Norway) and triphenyleno[1,12-*bcd*]thiophene ($C_{18}H_{10}S$) from the PAH Research Institute, Greifenberg, Germany (Marynowski et al., 2002). For maturation experiments, sufficient amounts of all four phenyldibenzothiophene isomers were obtained via free radical phenylation of dibenzothiophene. Freshly distilled aniline (0.01 mol DBT equiv., 0.09 mL) and pentyl nitrite (0.1875 mL; Merck), the source of phenyl radicals (Spagnolo et al., 1972), were mixed with dibenzothiophene (0.001 mol, 184 mg; Fluka, > 98%). The reaction mixture was homogenised by dissolving it in a minimal volume of dichloromethane (DCM) in a glass ampoule. After solvent evaporation to dryness at room temperature, the ampoule was sealed and kept at 40 °C for 2 days. The reaction products were extracted with benzene and dried. The residue was fractionated to give an aromatic fraction, which was used for our maturation experiments.

2.5. Maturation experiments

The maturation experiments with a clay catalyst, mimicking natural acid catalysed reactions (e.g. Wei et al., 2006), was conducted on a standard mixture (ca. 25 mg) of all four phenyldibenzothiophene isomers (see above), with the unstable 1- and 4-isomers prevailing (cf. Fig. 4c). The isomer mixture in DCM was adsorbed on to aluminium montmorillonite mixed with Cu powder [10:2; v/v; procedure adopted from Kagi et al. (1990) and Strachan et al. (1988)]. The clay has layers with a relative negative charge, so cations or protons (hydrated in the form of H_3O^+) are often located in the interlayer and on the surface (Moore and Reynolds, 1997). The solvent was evaporated and the mixture sealed at atmospheric pressure in glass ampoules, which were heated isothermally at 250 or 330 °C (1 week). After cooling, the reaction mixture was extracted with DCM and the solvent then allowed to evaporate at room temperature to give a residue, from which the fraction eluted with *n*-hexane/DCM (1:1; v/v) was analysed using GC–MS. The fraction contained all four phenyldibenzothiophenes, dibenzothiophene, biphenyl as major compounds, as well as traces (< 3% relativel to the sum of the phenyldibenzothiophenes) of benzophenone, phenanthrene, *m*- and *p*-terphenyls, xanthone, thiaxanthone, triphenyleno[1,12-*bcd*]thiophene and 2-phenylnaphthalene. Benzene and other low molecular products of pyrolysis were likely lost on work up.

2.6. Calculations

The geometry optimisation and calculation of thermodynamic properties for the dibenzothiophene derivatives were performed with the quantum chemical AM1 semi-empirical method (Dewar et al., 1985) and *ab initio* density functional theory (DFT) at B3LYP/6-31+G* level (Lee et al., 1988; Becke, 1993) using WinGamess'06 software (Schmidt et al., 1993) and Gaussian Inc. software (Frisch et al., 2004).

The composition of the thiophenes at equilibrium can be estimated on the basis of their thermodynamic properties, such as relative energy (ΔE), enthalpy (ΔH) or Gibbs free energy (ΔG), according to the following equation (e.g. van Duin et al., 1997):

$$\%C_i = 100 \cdot \frac{\exp\left(\frac{\Delta G_i - \Delta G_1}{RT}\right)}{1 + \sum_{n=2}^{N} \exp\left(\frac{\Delta G_n - \Delta G_1}{RT}\right)}$$

where N is the number of compounds and ΔG_1 is the Gibbs free energy of an arbitrarily chosen compound 1.

In order to predict kinetics for suspected natural reactions, potential energy surfaces were scanned in search of transition and intermediate structures, initially with the AM1 method. Then, all suspected equilibrium and transition structures were optimised under the AM1 level of theory. These structures were used as starting points for locating corresponding geometries at the B3LYP/6-31+G* level of theory. All transition states and equilibrium structures were verified by normal coordinate analysis. For each transition state, one imaginary (negative) frequency (ν) of the normal mode was found, the one that defines the transition state. For equilibrium structures all frequencies were positive. More exact energies were obtained employing single point B3LYP/6-311++G** calculations.

The polarisable continuum model (PCM) (Miertus et al., 1981) approach was used to study solvent effects. The gas phase B3LYP/6-31+G* optimised geometries were used as starting points to run single point PCM/B3LYP/6-311++G** calculations. Relative energies of species involved in the modelled reactions are expressed as $\Delta E_{(gas)}$ in the gas phase and $\Delta E_{(aq)}$ in aqueous solution. As solvents water under ambient (dielectric constant 78.4) and high temperature conditions at 300 °C and 500 bar (dielectric constant12.0) were used (e.g. Pitzer, 1983).

3. Results

3.1. Natural samples

For the geological samples, the relative abundances of phenyldibenzothiophenes (PhDBTs; Table 1) generally correlate well with R_r, except for the 4-isomer (Fig. 1). In Fig. 2, the outlier samples (Jaworznia, Poronin PAN-1) were omitted owing to their large R_r standard deviations (e.g. Środoń et al., 2006). In sections like Polkowice-Sieroszowice, several samples were collected within 2–3 m of a thick sedimentary sequence, so if only one sample contained vitrinite, its reflectance was considered for the others. In less mature samples, the most abundant isomers are either 1-PhDBT or 4-PhDBT, while 2- and 3-PhDBTs occur at comparable, but low, concentrations. In turn, the more mature samples contain 4-, 2- and 3-PhDBTs, which greatly prevail over 1-PhDBT. The concentration of 1-PhDBT rapidly decreases with increasing maturity and becomes essentially absent above R_r 0.9. For moderate maturity, 2-PhDBT pre-

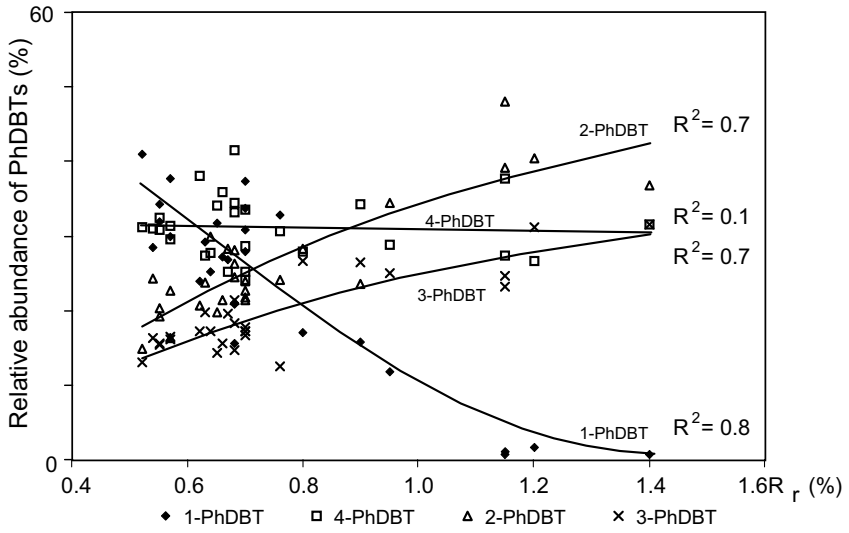

Fig. 1. Relative abundance of phenyldibenzothiophene isomers vs. mean vitrinite reflectance (R_r).

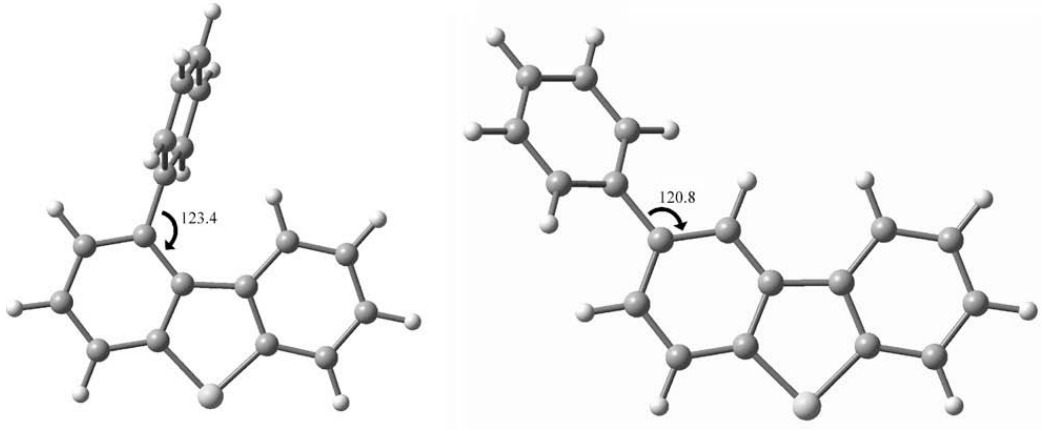

Fig. 2. Comparison of 1-phenyldibenzothiophene geometry, for which the angle between dibenzothiophene and phenyl moieties deviated from optimal to 123.4°, with 2-phenyldibenzothiophene geometry (B3LYP/6-31+G*).

vails over 3-PhDBT, while for higher maturity the proportion can be inversed, as in the hydrothermal oil from the Guaymas Basin [Fig. 6 from Marynowski et al. (2002)].

3.2. Thermodynamics

The calculations of either enthalpies or Gibbs free energies for the PhDBT isomers reveal that the most stable are 2- and 3-PhDBT, followed by 4-PhDBT and finally the least stable, 1-PhDBT (Table 2). The instability, resulting from the phenyl ring at C-1, is caused by steric hindrance (Fig. 2). For 1-PhDBT the angle between the phenyl and DBT moieties is deformed from the optimal 120°. This results in an increase in total energy and an overall instability. For comparison, the corresponding angle of 2-PhDBT, one of the most stable isomers, is less deformed (Fig. 2). The 1-PhDBT steric hindrance also causes the torsion angle between the phenyl ring and the DBT moiety to be twisted to about 90° (Fig. 2). The relative abundance of particular isomers in the thermodynamic equilibrium mixture obtained in the modelling (Table 2; Fig. 3) is comparable with the distribution of phenyldibenzothiophenes in samples with high maturity (e.g. Laskowa Góra, R_r 1.2%; Fig. 3). The distributions also compare well with that resulting from heating the mixture of all PhDBT isomers at 330 °C (Fig. 3). In addition, the presence of triphenyleno[1,12-*bcd*]thiophene, accompanied by the disappearance of 1-PhDBT, in mature samples suggests its formation from 1-PhDBT via cyclisation (Fig. 4), which is formally an oxidation. The amount of triphenyleno[1,12-*bcd*]thiophene estimated to be in thermodynamic equilibrium with PhDBT requires comparison of the thermodynamic properties such as, for example, relative enthalpy. However, as a result of the different elemental compositions, such a direct comparison is not possible. In order to compare the thermodynamic stability of triphenyleno[1,12-*bcd*]thiophene vs. phenyldibenzothiophenes, the enthalpy of all the substrates taking part in the cyclisation must be considered. Thus, the amount of triphenyleno[1,12-*bcd*]thiophene at such an equilibrium depends on the reaction mechanism leading to its formation. Many reaction mechanisms that involve different oxidants are theoretically possible but, as suggested from laboratory experiments (McCollom et al., 2001) and geological observations

Table 2
Comparison of thermodynamical properties of phenyldibenzothiophene isomers [enthalpy ΔH and free enthalpy (ΔG) are expressed relative to the most stable isomers]

Temperature	25 °C			330 °C		
Isomer	ΔH [kcal/mol]	S [cal/mol K]	ΔG [kcal/mol]	ΔH [kcal/mol]	S [cal/mol K]	ΔG [kcal/mol]
	Gas phase[a]					
1- PhDBT	3.79	120.89	3.14	3.79	179.95	2.47
2- PhDBT	0.17	118.74	0.16	0.17	177.79	0.15
3- PhDBT	0.00	118.71	0.00	0.00	177.75	0.00
4- PhDBT	1.13	118.83	1.10	1.13	177.87	1.06
	Aqueous solution[b]					
1- PhDBT	4.06	114.12	5.50	3.52	172.11	7.19
2- PhDBT	0.15	119.18	0.09	0.20	178.52	0.00
3- PhDBT	0.00	118.95	0.00	0.00	178.11	0.05
4- PhDBT	1.33	119.19	1.26	1.37	178.52	1.18

[a] B3LYP/6-31+G*.
[b] PCM/B3LYP/6-31+G*.

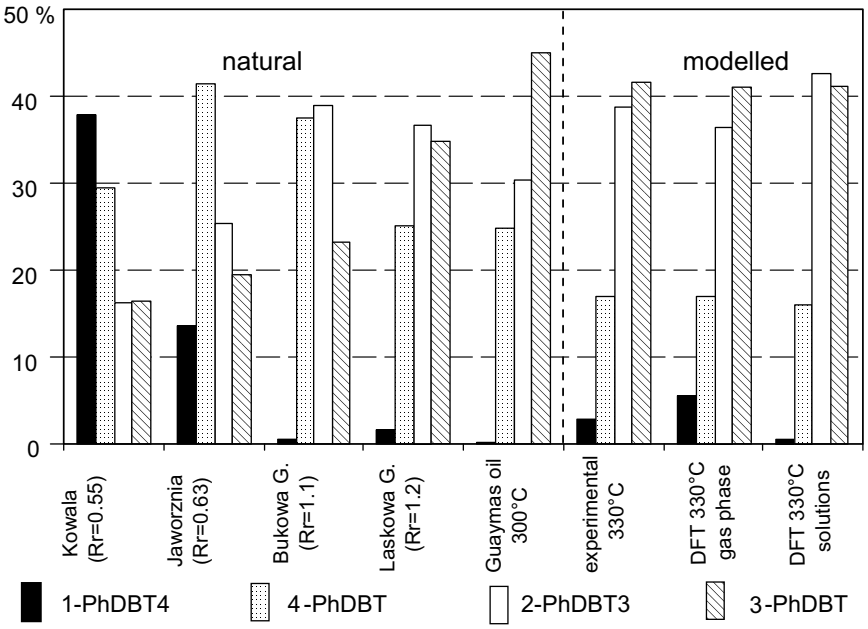

Fig. 3. Comparison of natural phenyldibenzothiophene distributions with experimental ones, and that predicted for thermodynamic equilibrium mixture.

(Graner and Warren, 1969; Xu et al., 1998), sulfur species are the most important agents promoting the transfer of electrons among reactants in many geological systems (Ohmoto and Lasaga, 1982, Seewald, 1997; McCollom et al., 2001; Zhang et al., 2008). The involvement of sulfur species at the intermediate oxidation state is consistent with the position of the investigated samples at the redox boundary, caused by a co-existence of metal sulfides (e.g. pyrite, chalcopyrite, bornite and chalccocite) and sulfates (anhydrite and gypsum) in the mineral matrix of the organic matter (e.g. Oszczepalski, 1989; Püttmann et al., 1990). Such a position for the investigated samples suggests involvement of simultaneous oxidation of sulfide–sulfur atoms and reduction of sulfate–sulfur. Given this, a mechanism of cyclisation involving thiosulfates, one of the important sulfur species in such environments (Ohmoto and Lasaga, 1982; Jørgensen, 1990; Xu et al., 1998; McCollom et al., 2001; Descostes et al., 2004; Zhang et al., 2007), was investigated in further detail:

$$\text{1-PhDBT} + HS_2O_3^- \rightarrow \text{TPT} + HSO_3^- + H_2S \quad (1)$$

The enthalpy of Reaction (1), calculated on the basis of energies, substrates and products is $\Delta E_{(aq)}$ ca. −21.0 kcal/mol (according to the PCM/B3LYP/6-31+G*//PCM/B3LYP/6-311++G** calculations). The reaction is quite exothermic, indicating that the thermodynamic stability of triphenyleno[1,12-*bcd*]thiophene (TPT) is substantially greater than that of the phenyldibenzothiophenes. If thermodynamic equilibrium were obtained, an enormous predominance (>99%) of triphenyleno[1,12-*bcd*]thiophene would be expected. This is not the case in nature (Fig. 4), suggesting that the compounds do not reach thermodynamic equilibrium, even in the hydrothermal petroleum from the Guyamas Basin (Marynowski et al., 2002) formed above 300 °C and at least 200 bar (Kawka and Simoneit, 1990; Simoneit, 1993).

3.3. Kinetics

In order to gain further insight into the way phenyldibenzothiophenes are transformed in geological environments, the kinetics of two reactions were evaluated: cyclisation of 1-PhDBT and isomerization of PhDBTs. These

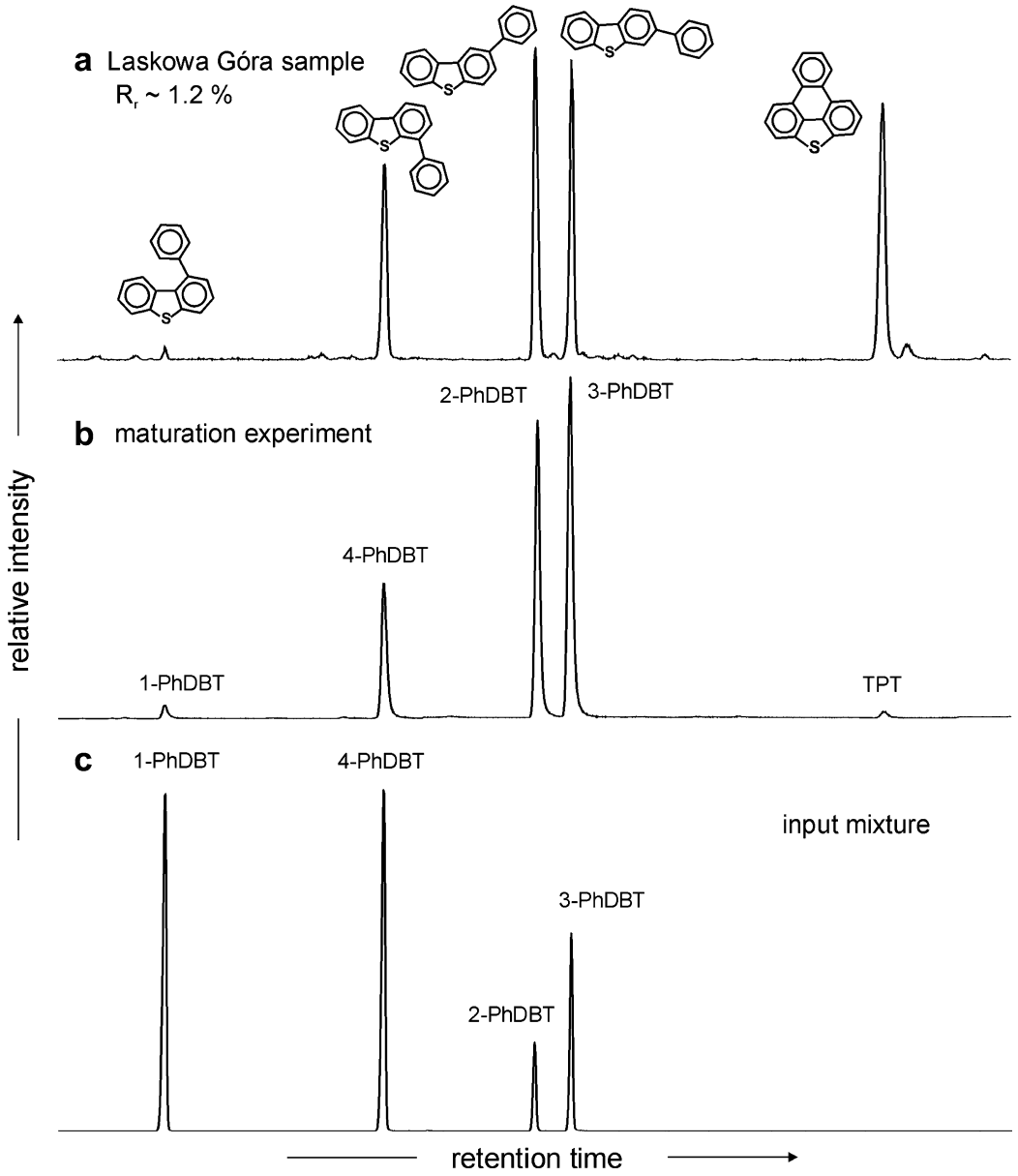

Fig. 4. Comparison of phenyldibenzothiophene and triphenyleno[1,12-*bcd*]thiophene distributions in: (a) mature rocks ($R_r \sim 1.2\%$), (b) products of laboratory maturation experiment at 330 °C resulted from heating, and (c) phenyldibenzothiophenes mixture obtained from free radical phenylation of dibenzothiophene as revealed by m/z 260 + 258 chromatograms.

reactions were suspected to go on in nature, on the basis of the identification of their presumed products in the geological samples and the maturation experiment.

3.3.1. Cyclisation of 1-phenyldibenzothiophene

It is noteworthy that 1-PhBDT can cyclise to TPT. This is caused by the specific TPT geometry, which differs from 1-PhDBT only in possessing one additional C–C bond, causing a lack of two hydrogens. The positions of the other C–C bonds are similar, which is not the case for the other PhDBTs. However, the other isomers can potentially form TPT, if they are first isomerised to 1-PhDBT (Section 3.3.2).

Non-catalytic cyclisation of 1-PhDBT has a high reaction barrier $\Delta E_{(gas)}$ ca. 72.4 kcal/mol. The acid catalysed scenario leads to a substantial increase in the relative stability of the intermediate molecule ($\Delta E_{(gas)}$ ca. 48.4 kcal/mol). The involvement of acid catalysis in diagenetic/catagenetic transformation of sedimentary organic matter has been widely anticipated, traditionally with the involvement of Lewis acids (e.g. Seewald et al., 2000; Wei et al., 2006). However, any strong acid could catalyse the cyclisation reaction. In sedimentary basins, acidic H^+ could originate from e.g. pyrite oxidation, hydrolysis of $MgSO_4$ (Janecky and Seyfried, 1983; Zhang et al., 2008) or from auto-dissociated high temperature water with higher H^+ and OH^- activities under hydrothermal conditions (e.g. Akiya and Savage, 2002; Seewald, 2003). To validate whether such a mechanism of dehydrocyclisation of 1-PhDBT to TPT, involving thiosulfate as oxidant [used in experiments by Toland (1960)], is realistic for geological conditions, all the molecules involved in such a reaction were fully optimised and three transition structures were located. The inclusion of acids in quantum chemical modelling was obtained by using H_3O^+, which during reaction, loses a proton

and becomes H_2O. In turn, the dominant thiosulfate species, $HS_2O_3^-$, in acidic aqueous solutions (Ohmoto and Lasaga, 1982) was used.

The construction of the potential energy surface (Fig. 5) for the acid catalysed reaction, analogous to (1), requires the inclusion of all substrates and products. In order to obtain the relative energy of particular molecules along the reaction path, all molecules taking part in the reaction were included in the calculations (Table 3). Thus, the overall reaction can be written as:

$$\begin{aligned}
&\text{1-PhDBT} + H_3O^+ + H_2O + HS_2O_3^- \\
&\quad \rightarrow \text{1-Int} + 2H_2O + HS_2O_3^- \rightarrow \text{TS1} + 2H_2O + HS_2O_3^- \\
&\quad \rightarrow \text{2-Int} + 2H_2O + HS_2O_3^- \\
&\quad \rightarrow \text{3-Int} + H_3O^+ + H_2O + HS_2O_3^- \\
&\quad \rightarrow \text{TS2} + H_2O + H_3O^+ \\
&\quad \rightarrow \text{4-Int} + H_2O + H_3O^+ + HSO_3^- \\
&\quad \rightarrow \text{TS3_HS} + H_2O + H_3O^+ + HSO_3^- \\
&\quad \rightarrow \text{5-Int} + HS^- + H_2O + H_3O^+ + HSO_3^- \\
&\quad \rightarrow \text{TPT} + HS^- + 2H_3O^+ + HSO_3^- \\
&\quad \rightarrow \text{TPT} + H_2S + H_2O + H_3O^+ + HSO_3^- \qquad (2)
\end{aligned}$$

Based on these assumptions, the first step is proton attack at C-4 of 1-PhDBT and the formation of an arenium ion 1-Int (Fig. 5). At all other positions, relative energies between particular intermediate protonated structures were not found to be substantial (about 2.0 kcal/mol according to the B3LYP/6-31+G* calculations). Indeed, proton attack at position 4 is most plausible, because it leads to the 1-Int privileged intermediate, which in further reaction steps acts as an electrophile and in intramolecular mode attacks other aromatic rings. It was also found that the reaction of

Table 3
Total energy of species in cyclisation of 1-phenyldibenzothiophene to triphenyleno[1,12-*bcd*]thiophene (transition stages are characterised by their imaginary frequencies)

Molecule	Gas phase[a]		Aqueous solution[b]	
	Imaginary frequency $\nu_{(gas)}$ (cm^{-1})	Total energy (Hartree)	Imaginary frequency $\nu_{(aq)}$ (cm^{-1})	Total energy (Hartree)
1-PhDBT		−1091.549952		−1091.563136
1-Int		−1091.878789		−1091.954159
TS1	−415	−1091.839049	−420[c]	−1091.914110
2-Int		−1091.853367		−1091.928473
3-Int		−1091.521031		−1091.534265
TS2	−63	−2114.280556	−170[c]	−2114.364360
4-Int		−1489.735251		−1489.752377
TS3	−341	−1489.684541		
TS3_HS			−142[c]	−1489.714488
5-Int				−1090.750813
TPT		−1090.363957		−1090.377309
$HS_2O_3^-$		−1022.805515		−1022.904318
HSO_3^-		−624.590145		−624.695639
H_2S		−399.422640		−399.427954
HS^-				−398.966595

[a] B3LYP/6-31+G*//B3LYP/6-311++G**.
[b] B3LYP/6-31+G*//PCM/B3LYP/6-311++G**.
[c] PCM/B3LYP/6-31+G*//PCM/B3LYP/6-311++G**.

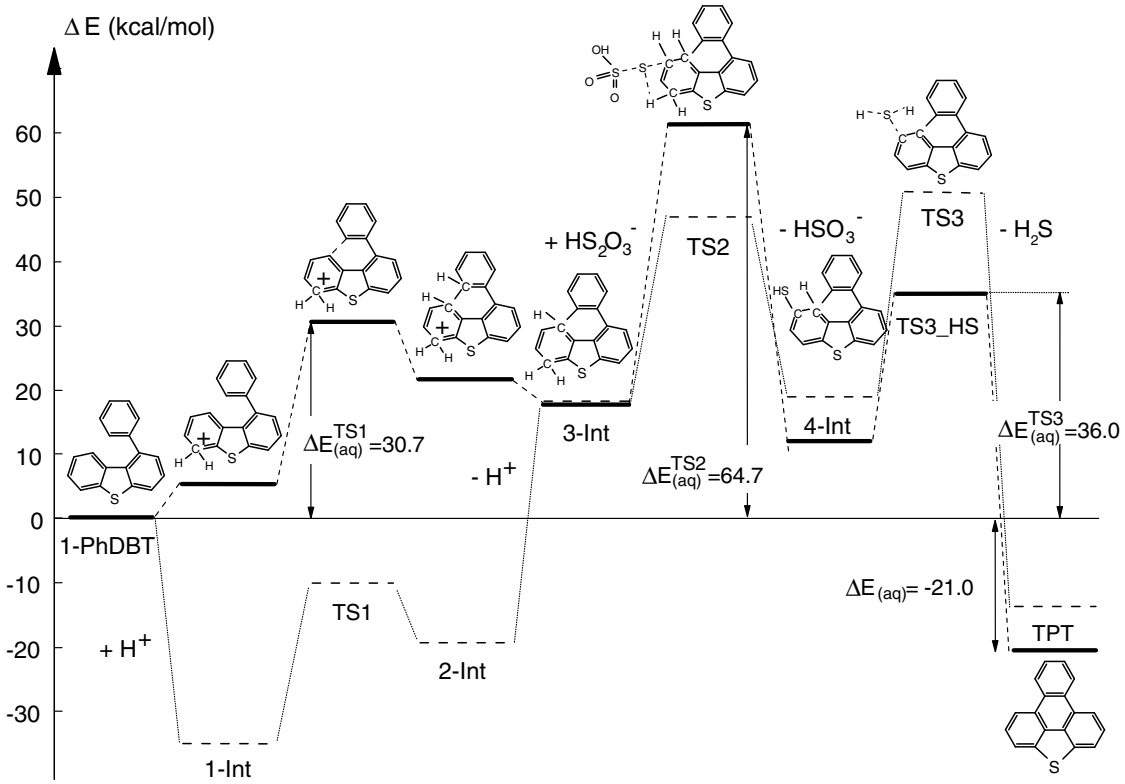

Fig. 5. Comparison of energy profile diagrams for dehydrocyclisation of 1-phenyldibenzothiophene to triphenyleno[1,12-*bcd*]thiophene by acid catalysis with involvement of thiosulfate in gas phase (dashed lines – B3LYP/6-31+G*//B3LYP/6-311++G**) and in aqueous solutions (solid lines – B3LYP/6-31+G*//PCM/B3LYP/6-311++G**).

a proton accession to 1-PhDBT has almost no barrier (ca. 4 kcal/mol – B3LYP/6-31+G*), so calculations of such potential barriers were omitted.

Within the context of the suggested acid catalysed reactions involving ionic species, the model may require due consideration of the solvation energy, which usually plays a significant role in the final energy (e.g. Jensen, 2001). Taking the first step in Reaction (2), which is 1-PhDBT + H_3O^+ → 1-Int + H_2O, in the gas phase H_3O^+ will be very unstable, which makes the right-hand side relatively more stable than it would be in aqueous solution. However, the solvation energy term for H_3O^+ will be very large. Although, 1-Int is also positively charged, the solvation energy term will be substantially smaller. This is because the positive charge in 1-Int will be well distributed in the aromatic rings particularly. Consequently, much less formation of 1-Int can be anticipated in aqueous solution than in the gas phase. To form 1-Int in the gas phase, a value of ca. −35 kcal/mol was obtained (Table 4). This would mean that 1-PhDBT is not stable at all, revealing that such a model is not applicable to naturally occuring diagenetic reactions. Therefore, results from the calculations in aqueous solution must be considered. For such circumstances the protonated forms like 1-Int, TS1 and 2-Int turn out to be relatively less stable than neutral 1-PhDBT as expected.

The first transition state TS1 (Appendix B) refers to the cyclisation of a protonated 1-PhDBT (1-Int) molecule. The cyclisation barrier obtained, $\Delta E^{TS1}_{(aq)}$ ca. 30.7 kcal/mol ($\Delta E^{TS1}_{(gas)}$ ca. 24.9 kcal/mol), seems realistic for geological conditions. The normal mode of the TS1 is characterised by one imaginary frequency at $\nu_{(aq)} = -420\ cm^{-1}$ in aqueous solution ($\nu_{(gas)}$ −415 cm^{-1} in gas phase) confirming the identification of the transition state. After crossing the barrier, the formed cationic 2-Int molecule (Figs. 5 and 6) possesses three additional hydrogens in comparison to TPT. One of them can be liberated in the form of H^+ and the molecule becomes neutral. At this step, the most distant hydrogen from the sulfur atom, the one between the two rings, is preferentially lost (in Fig. 6, arrow). This is attributed to the loss of aromaticity from only two rings, instead of three, as would be the case for other protons. This leads to a relative lowering of energy in respect of the 3-Int molecule (Fig. 5). If the proton were liberated from other positions, the energy of such molecules would be higher by about 40–60 kcal/mol.

At this stage, the neutral 3-Int molecule with two additional protons (Fig. 5) is attacked by model oxidant, thiosulfate $HS_2O_3^-$. Thiosulfate, though formally contains sulfur S^{4+}, is a hybrid species consisting of two non-equivalent sulfur atoms. Sulfate-type sulfur S^{6+} of the thiosulfate is reduced to S^{4+} and sulfide-type sulfur S^{2-} is added to the molecule 3-Int. The second transition state TS2 (Appendix B), characterised by one imaginary frequency at $\nu_{(aq)}$ −170 cm^{-1} ($\nu_{(gas)}$ −63 cm^{-1}), refers to such an addition. The formation of TS2 requires $\Delta E^{TS2}_{(aq)} = 64.7$ kcal/mol ($\Delta E^{TS2}_{(gas)} = 47.0$ kcal/mol; Table 3), which suggests that the reaction is likely to proceed only at advanced diagenesis/catagenesis. This transition state is quite a complex one, because it requires the formation of two new bonds accompanied by the breaking of two others (see Appendix B). In our modelling, it is difficult to ascertain whether or not no other transition states are possible, due to limitations in transition state computations (e.g. Jensen, 2001). However, TS2 was the only transition structure, obtained after several trials, that is intermediate between TPT with two additional hydrogens (structure 3-Int, Fig. 5) and TPT with hydrogen and SH group (4-Int, Fig. 5). The TS2 liberates the HSO_3^-, thereby forming the 4-Int structure. The latter differs from TPT in having an additional hydrogen and hydrosulfide group.

In aqueous solution 4-Int preferably loses hydrosulfide ion HS^-, via a transition state TS3_HS (Appendix B) identified due to the finding of one imaginary frequency of the normal mode at $\nu_{(aq)} = -142\ cm^{-1}$ and becomes an arenium ion 5-Int (Fig. 5). H^+ is then liberated and the molecule becomes neutral TPT. Hydrosulfide ions can be stable in aqueous solution under certain pH values, but the molecular modelling is still unable to computationally consider the pH of aqueous solutions (Jensen, 2001). Therefore, exclusively for the purpose of the modelling hydrosulfide ion was assumed to recombine with hydronium ion:

$$HS^- + H_3O^+ \rightarrow H_2S + H_2O$$

leading to a lowering of the total energy. For the reason mentioned, the last steps ($5\text{-Int} + HS^- + H_2O + H_3O^+ + HSO_3^- \rightarrow TPT + HS^- + 2H_3O^+ + HSO_3^- \rightarrow TPT + H_2S + H_2O + H_3O^+ + HSO_3^-$) in Reaction (2) resulting from the methodological limitations are only shown in Tables 3 and 4 (omitted from Fig. 5). For the gas phase the final reaction steps would be quite different. After crossing the TS3 transition state (Appendix B), H_2S is liberated from 4-Int, rather than HS^-. Finding one imaginary frequency of the normal mode at $\nu_{(gas)} = -341\ cm^{-1}$ identifies TS3. Eventually, as in aqueous solution, TPT molecule is formed.

3.3.2. Isomerization of PhDBTs

It is generally accepted that methyl (e.g. Strachan et al., 1988; Kagi et al., 1990) and phenyl (Marynowski et al., 2002; Rospondek et al., 2007) groups can easily migrate round aromatic rings. For example, it has been shown experimentally that upon heating *o*-terphenyl isomerises, yield both the *m*- and *p*-isomers (Marynowski et al.,

Table 4
Energy calculated for cyclisation of 1-phenyldibenzothiophene to triphenyleno[1,12-*bcd*]thiophene (energy expressed relative to substrates)

Molecule	1-PhDBT	1-Int	TS1	2-Int	3-Int	TS2	4-Int	TS3	TS3_HS	5-Int	TPT + HS^-	TPT
Energy	ΔE (kcal/mol)											
Gas phase[a]	0.0	−35.3	−10.4	−19.3	18.1	47.0	18.9	50.7				−13.3
Solution[b]	0.0	5.6	30.7[c]	21.7	18.1	64.7[c]	12.2		36.0[c]	34.1	17.6	−21.0

[a] B3LYP/6-31+G*//B3LYP/6-311++G**.
[b] B3LYP/6-31+G*//PCM/B3LYP/6-311++G**.
[c] PCM/B3LYP/6-31+G*//PCM/B3LYP/6-311++G**.

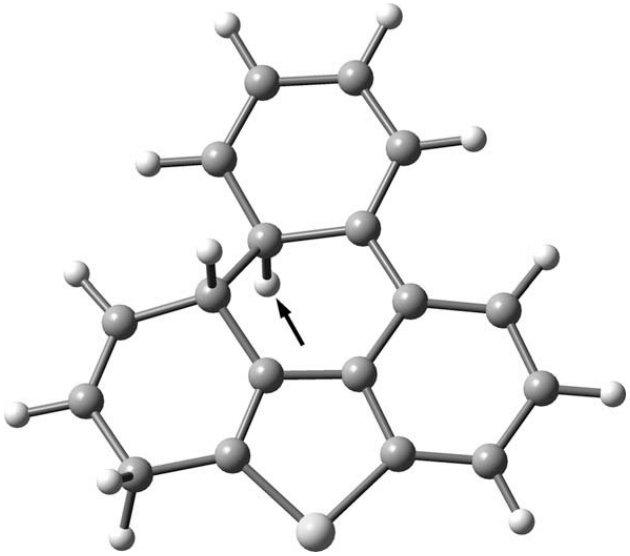

Fig. 6. Structure of cationic 2-Int showing the preferred position of proton liberation (arrow) (B3LYP/6-31+G*).

2001). In order to check whether the mechanism of isomerisation of phenyldibenzothiophenes has a low activation energy, transition state calculations were performed for the gas phase ($\Delta E_{(gas)}$) and aqueous solution ($\Delta E_{(aq)}$). Again, it was presumed that the mechanism is acid clay catalysed (e.g. montmorillonite was employed for mimicking natural environments). The potential energy surface for one of the isomerization reactions e.g. (3)

$$\text{1-PhDBT} \rightarrow \text{2-PhDBT} \quad (3)$$

can be obtained by including all the reactants involved in Reaction (3):

$$\begin{aligned}&\text{1-PhDBT} + H_3O^+ \rightarrow \text{1-PhHDBT}^+ + H_2O\\ &\rightarrow \text{TS1}{-}2 + H_2O \rightarrow \text{2-PhHDBT}^+ + H_2O\\ &\rightarrow \text{2-PhDBT} + H_3O^+ \end{aligned} \quad (4)$$

The results of the calculations for all molecules (Table 5) were used to constrain the potential energy surfaces (Table 6, Fig. 7). The first step is proton attack at C-1 of 1-PhDBT, subsequently leading to a hybridisation change from sp^2 to sp^3. Proton attack at any other position does not allow isomerisation to proceed. In the gas phase, the negative $\Delta E_{(gas)}$ value of ~−30 kcal/mol (Table 6) was obtained for the protonation of 1-PhDBT to form the arenium ion 1-PhHDBT$^+$. This would mean again that 1-PhDBT is not stable at all, which is not a realistic model for natural conditions, and this acid-catalysed reaction must be modelled in aqueous solution. Then, neutral forms like 1-PhDBT and 2-PhDBT turn out to be relatively more stable than the corresponding 1-PhHDBT$^+$ and 2-PhHDBT$^+$ arenium ions.

The activation energy $\Delta E_{(aq)}$ of isomerisation ranges from 20.5 to 28.7 kcal/mol ($\Delta E_{(gas)}$ from 13.6 to 19.0 kcal/mol) (Table 6). For example, Reaction (4) barrier $\Delta E_{(aq)}^{TS1-2}$ has ca. 20.5 kcal/mol ($\Delta E_{(gas)}^{TS1-2}$ 13 kcal/mol) (Fig. 7). These barriers can be easy to overcome at relatively low temperature in natural environments.

The atomic displacement vectors of the normal mode of the transition state TS1–2 (Fig. 8), characterised by the imaginary (negative) frequency at $\nu_{(aq)} = -270\ cm^{-1}$ ($\nu_{(gas)} = -313\ cm^{-1}$), confirm that the TS1–2 structure (Appendix B) corresponds to the transitional geometry between two neighbouring structures: 1-PhHDBT$^+$ and 2-PhHDBT$^+$. Other isomerisations proceed according to the mechanism, by analogy with that described for the 1-PhDBT → 2-PhDBT reaction. The imaginary frequencies of the normal modes defining the transition states of the two other isomerisation reactions are: TS2–3 at $\nu_{(aq)} = -344\ cm^{-1}$ ($\nu_{(gas)} = -376\ cm^{-1}$) and TS3–4 at $\nu_{(aq)} = -280\ cm^{-1}$ ($\nu_{(gas)} = -322\ cm^{-1}$).

4. Discussion

4.1. Geological implications of phenyldibenzothiophene isomerisations

Phenyldibenzothiophenes have been detected generally only in rocks with low organic matter content (Table 1). Relatively high fluid to solid mass ratios during such rocks diagenesis/catagenesis limited reducing capacity of the rocks leading to the formation of phenylated PACs includ-

Table 5
Total energy of species in phenyldibenzothiophene isomerisation (transition stages are characterised by their imaginary frequencies)

Molecule	Gas phase[a]		Aqueous solution[b]	
	Imaginary frequency $\nu_{(gas)}$ (cm^{-1})	Total energy (Hartree)	Imaginary frequency $\nu_{(aq)}$ (cm^{-1})	Total energy (Hartree)
1-PhDBT		−1091.549952		−1091.563136
1-PhHDBT$^+$		−1091.874259		−1091.951541
TS1–2	−313	−1091.852601	−270[c]	−1091.930408
2-PhHDBT$^+$		−1091.877453		−1091.956383
2-PhDBT		−1091.555377		−1091.570135
TS2–3	−376	−1091.847098	−344[c]	−1091.924343
3-PhHDBT$^+$		−1091.876993		−1091.954859
3-PhDBT		−1091.555375		−1091.570129
TS3–4	−322	−1091.851601	−280[c]	−1091.929171
4-PhHDBT$^+$		−1091.874531		−1091.953375
4-PhDBT		−1091.553937		−1091.568279
H_2O		−76.458434		−76.472383
H_3O^+		−76.731019		−76.872255

[a] B3LYP/6-31+G*//B3LYP/6-311++G**.
[b] B3LYP/6-31+G*//PCM/B3LYP/6-311++G**.
[c] PCM/B3LYP/6-31+G*//PCM/B3LYP/6-311++G**.

Table 6
Calculated energy for phenyldibenzothiophene isomerisations relative to energy of each initial structure (calculated energy are related to each initial structure)

Energy	Initial structure	Protonated initial structure	Transition state	Protonated final structure	Final structure	Energy barrier
	ΔE (kcal/mol)					
	1-PhDBT	1-PhHDBT$^+$	TS1–2	2-PhHDBT$^+$	2-PhDBT	
Gas phase[a]	0.0	−32.5	−18.9	−34.5	−3.4	13.6
Solution[b]	0.0	7.2	20.5	4.2	−4.4	20.5
	2-PhDBT	2-PhHDBT$^+$	TS2–3	3-PhHDBT$^+$	3-PhDBT	
Gas phase[a]	0.0	−31.1	−12.0	−30.8	0.0	19.0
Solution[b]	0.0	8.5	28.7	9.5	0.0	28.7
	3-PhDBT	3-PhHDBT$^+$	TS3–4	4-PhHDBT$^+$	4-PhDBT	
Gas phase[a]	0.0	−30.8	−14.8	−29.2	0.9	15.9
Solution[b]	0.0	9.5	25.7	10.4	1.2	25.7

[a] B3LYP/6-31+G*//B3LYP/6-311++G**.
[b] B3LYP/6-31+G*//PCM/B3LYP/6-311++G**.

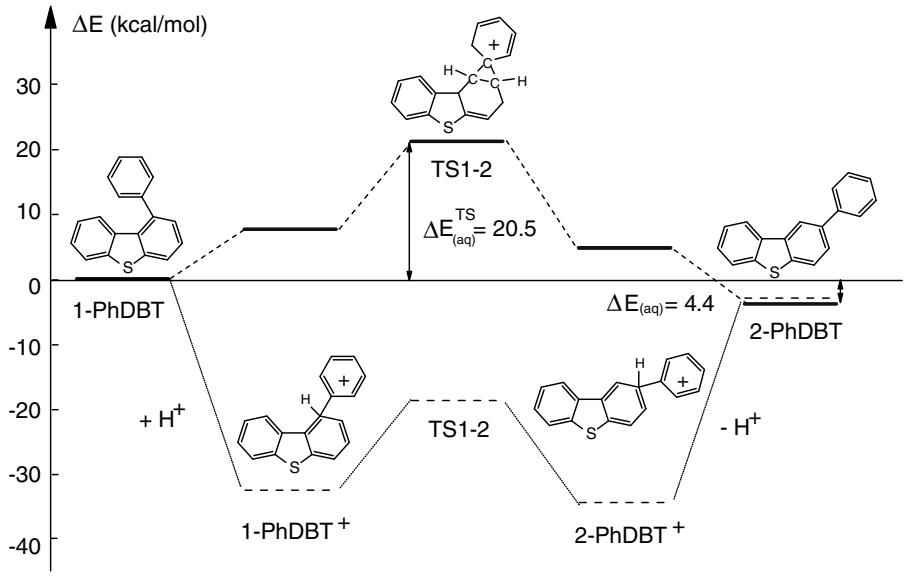

Fig. 7. Comparison of energy profile diagram for isomerisation of 1- to 2-phenyldibenzothiophene in gas phase (dashed lines – B3LYP/6-31+G*//B3LYP/6-311++G**) and in aqueous solutions (solid lines – B3LYP/6-31+G*//PCM/B3LYP/6-311++G**).

ing phenyldibenzothiophenes (Rospondek et al., 2007). The low maturity samples, containing all four isomers and with a dominance of 1- and 4-PhDBT, are thermodynamically unstable (Figs. 1 and 3), while with increasing maturity the composition begins to resemble that of the thermodynamic equilibrium, with the 2- and 3-PhDBTs dominant (Fig. 3). Analysis of all the available data on the phenyldibenzothiophene distribution (Table 1) shows that the isomer abundance is clearly dependent, with the exception of the 4-isomer, on maturity expressed as vitrinite reflectance (Figs. 1 and 3). The vitrinite reflectance for the analysed rock sequences is frequently characterised by rapid variation within a few meters (e.g. Sawłowicz, 1993), which strongly suggests that vitrinite records not only thermal gradient but that there are more likely differences in pH and redox conditions, as experimentally demonstrated by Seewald (1997) and Seewald et al. (2000). Their experiment on the role of aqueous fluid and sediment composition, and timing on the development of vitrinite reflectance at elevated temperatures, pointed to a significant role of acid catalysis. The results of our maturation experiment and molecular modelling of PhDBTs distributions also suggest the importance of acid catalysis in processes involved in the evolution of molecular maturity parameters based on phenyldibenzothiophenes. For PhDBT isomerisation, a 1,2-phenyl shift was studied in detail as one of the plausible mechanisms governing the evolution of the phenyldibenzothiophene ratio, by analogy with the widely described 1,2-methyl shift (e.g. Strachan et al., 1988; Kagi et al., 1990). Indeed, only when the initial step is acid catalysed, is the activation energy $\Delta E_{(aq)}$ ca. 20.5–28.7 kcal/mol modelled (Table 6, Fig. 9). Such a low barrier is consistent with the observation of increasing amounts of the more stable isomers at the expense of the less stable ones, beginning from the very early stages of oil generation (Fig. 1). Closer inspection of the barrier variations for each of the isomerisations reveals that 1-PhDBT is able to isomerise to 2-PhDBT easily, as a result of the $\Delta E_{(aq)}$ ca. 20.5 kcal/mol barrier, while the reaction from 2- to 3-PhDBT is more difficult to occur, because of the higher barrier $\Delta E_{(aq)}$ ca. 28.7 kcal/mol (Figs. 7 and 9). The difference means that, in the 2- to 3-PhDBT isomerisation reaction, the same rate of phenyl shift could be roughly achieved at a temperature of ca. 150 °C higher than for the 1- to 2-

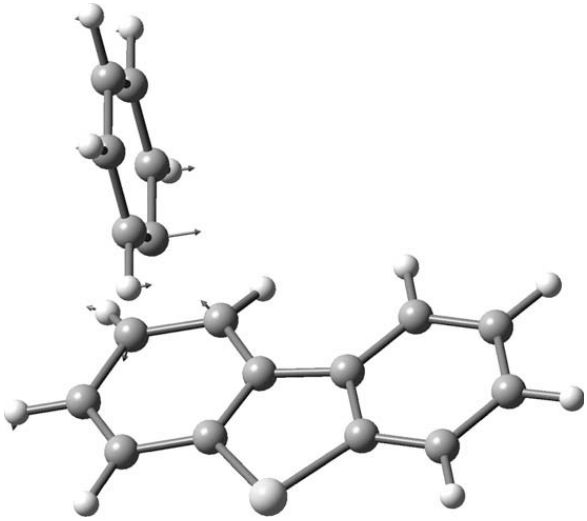

Fig. 8. Atomic displacement vectors (arrows) of the arenium transition state TS1–2 for acid catalysed phenyldibenzothiophene isomerisation (B3LYP/6-31+G*).

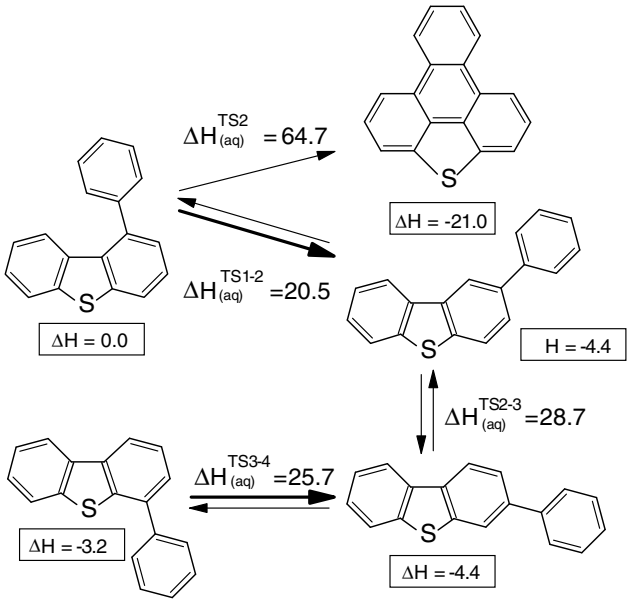

Fig. 9. Suspected transformations of phenyldibenzothiophenes in nature. Thicker arrows indicate preferable isomerisation reactions at the onset of maturation, however, once the conditions are fulfilled at very advances stages of maturity cyclisation gains in significance. ΔH is relative difference in enthalpy between particular isomers and ΔH^{TS} activation energy for acid catalysed isomerisations in aqueous solutions (kcal/mol).

PhDBT isomerisation. This is likely the reason for the observed persistence of the 2-isomer over 3-PhDBT up to the late stages of the oil generation window (Figs. 1 and 3). In the most mature samples, 2- and 3-PhDBTs can be found in similar amounts and, likewise, in the products of the maturation experiment (Figs. 3 and 4), suggesting that under such conditions all phenyl shift barriers can easily be overcame. The likely reason for the encountered predominance of the 3- over 2-isomer in some mature samples (Fig. 1), such as in the hydrothermal Guaymas oil (Fig. 3), could be the preferential formation of the 3-isomer exclusively from the 4-isomer, because at advanced maturity levels 1-PhDBT is not present. A higher than expected concentration of 4-PhDBT in mature samples and its poor correlation with vitrinite reflectance cannot be easily explained on the basis of our data, but may result from, for example, high generation rates from kerogen at advanced stages of diagenesis/catagenesis or from a shielding effect; hence, its different behaviour during migration (e.g. Oldenburg et al., 2002).

Interestingly, in geological samples with very low maturity (e.g. Kowala, $R_r \sim 0.55\%$) considerable amounts of both 1- and 4-PhDBT were found, together with minor amounts of other isomers. The conversion from 1-PhDBT to 4-PhDBT seems possible only at more advanced stages of diagenesis/catagenesis (Fig. 9). However, this would have to lead to the equilibrium composition, which is not observed (Fig. 1). Therefore, all PhDBT isomers must have been formed together at the earliest stages of diagenesis. Consequently, the formation of the other three isomers, especially 4- from 1-PhDBT, the only isomer possessing a linear carbon skeleton (Rospondek et al., 2007), via the phenyl shift mechanism seems unlikely (Fig. 9). Unfortunately, the studied processes do not shed light on the mechanisms of phenyldibenzothiophenes formation in nature, which could explain the poor correlation of 4-PhDBT amounts with maturity (Fig. 1). The described process of phenyldibenzothiophenes formation starts from their asymmetrical structural isomers, i.e. phenylnaphtho[*b*]thiophenes and naphthylbenzo[*b*]thiophenes, which are present in relatively higher concentrations with them at about the threshold of oil generation (ca. R_r 0.5) and which later quickly decay. This is concluded from the fact that PhDBTs were formed upon artificial heating of phenylnaphtho[*b*]thiophene standards (Rospondek et al., 2007). They also form as pyrolytic products from dibenzothiophene (Dartiguelongue et al., 2006) as well as from coal tars and pitches (Meyer zu Reckendorf, 2000).

The evaluation of the processes that govern the distribution of the DBT derivatives in geological samples has some implications for the application of the maturity parameters based on these derivatives (Radke and Willsch, 1994; Radke et al., 1986, 2000; Chakhmakhchev et al., 1997; Marynowski et al., 2002). While in mature samples, the 2- and 3-isomers are dominant among the PhDBTs (Table 1; Figs. 1 and 3), this is never the case for methyldibenzothiophenes, finally dominated by the 4-isomer (Radke and Willsch, 1994; Radke et al., 1986; Chakhmakhchev et al., 1997). The discrepancy is reflected in the empirical selection of different isomers for the methyl- and phenyldibenzothiophene maturity parameters. The most commonly used, the methyldibenzothiophene ratio (MDR) was defined as the ratio of 4-/1-MeDBT concentrations (Radke et al., 1986), and later redefined as 4-MeDBT/(4- + 1-MeDBT) (Radke and Willsch, 1994), while the phenyldibenzothiophene ratio was defined as 2-PhDBT/(2- + 1-PhDBT) (Marynowski et al., 2002). The common choice of the 1-isomer for both parameters resulted from the observed decrease in 1-PhDBT concentration, similar to the drop in 1-methyldibenzothiophene concentration (Radke et al., 1986) and in 1-alkyl isomers in general (van van Aarssen et al., 2001) with increasing maturity. In turn, a high level of maturity correlating well the behaviour of the 4-alkyl isomer contrasts with that of 4-PhDBT (Radke and Willsch, 1994; Chakhmakhchev et al., 1997), which

hardly correlates with maturity (Fig. 1). Accordingly, this has resulted in the choice of 2-PhDBT for the phenyldibenzothiophene ratio. A direct comparison of both maturity indicators is precluded by the fact that both compound groups have not been found together in the same rocks. All this reveals that, for the same level of OM maturity, the distribution of alkyl and phenyl derivatives can differ. A shielding effect is suggested to be the important factor controlling the distribution of polar aromatic compounds like xanthones in oils (Oldenburg et al., 2002) and may play a role in the persistence of 4-MeDBT in the geosphere. Further studies are needed to explain reasons for the major differences in both derivative compositions. An indirect insight into the cause of such differences can be gained from the molecular modelling of kinetic barriers for MeDBT and PhDBT isomerisations.

4.2. Geological implications of phenyldibenzothiophene cyclisation

At very advanced stages of diagenesis/catagenesis (also termed epigenesis, e.g. Püttmann and Villar, 1987; Püttmann et al., 1990), 1-PhDBT dehydrocyclisation to TPT can gain in importance (Marynowski et al., 2002; Rospondek et al., 2007), assuming the proposed mechanism of this reaction (Reaction (2)), the formation of the cyclic product from 1-PhDBT, must depend on the availability of energy and oxidants. For the model oxidant (see discussion in Section 3.2), thiosulfate was used [also used in experiments by Toland (1960)], the reaction is exothermic $\Delta E_{(aq)}$ ca. −21 kcal/mol (Fig. 9), meaning that the balance is shifted significantly towards the cyclic product. If the thermodynamic equilibrium between phenyldibenzothiophenes and TPT were reached in nature, TPT would be the most abundant compound in such a mixture. This is not the case (Fig. 4), but in highly mature samples like Laskowa Góra (Fig. 4a), it is indeed an abundant compound. If acid catalysed cyclisation of 1-PhDBT with thiosulfate as oxidant (Toland, 1960) is modelled, the overall activation barrier is $\Delta E_{(aq)}$ ca. 64.7 kcal/mol (Figs. 5 and 9). Under such conditions, re-isomerisations from 4-, 3- and 2- to 1-PhDBT occur frequently due to low barriers ($\Delta E_{(aq)}$ 20.5–28.7 kcal/mol). Then, the 1-PhDBT can be considered as an unstable intermediate on the cyclisation reaction path. A summary of the calculated relative enthalpies (ΔH) and energy barriers (ΔE^{TS}) for phenyldibenzothiophene isomerisations and dehydrocyclisation is shown in Fig. 9. At such stages, fluid temperatures can be substantially elevated, e.g. to 300 °C, leading to a drastic shift in physical properties of water, like that carrying hydrothermal petroleum in the Guaymas Basin (Kawka and Simoneit, 1990; Simoneit, 1993). The dielectric constant of water falls significantly (e.g. Pitzer, 1983) and oils become more fluid soluble. For such fluids, the modelled energy barrier of the cyclysation can be lowered by ca. 2–3 kcal/mol (PCM/B3LYP/6-31+G*//PCM/B3LYP/6-311++G**).

Interestingly, the energy obtained for the rate limiting cyclisation barrier is comparable with the barrier (ca. 56 kcal/mol) calculated for thermochemical sulfate reduction (TSR; Ellis et al., 2007). TSR has often been proposed as the major process controlling redox reactions during metal precipitation and oxidation of organics in the Kupferschiefer samples (for a discussion, see Püttmann et al., 1990; Bechtel et al., 2001, 2002). TSR leads to extensive oxidation of hydrocarbons to CO_2 and formation of water, but also promotes aromatisation of organic matter. The process is enhanced by the initial presence of H_2S (e.g. Goldhaber and Orr, 1995; Ellis et al., 2007). The choice of thiosulfate for modelling, the species generated at the redox boundary, in reaction (Ohmoto and Lasaga, 1982):

$$H_2S + SO_4^{2-} \rightleftarrows S_2O_3^{2-} + H_2O \quad (5)$$

is attractive, because it gives the chance to regenerate H_2S with organic matter (e.g. *o*-terphenyl to give triphenylene) [Reaction (6)]:

$$S_2O_3^{2-} + C_{18}H_{14} \rightarrow SO_3^{2-} + H_2S + C_{18}H_{12} \quad (6)$$

and subsequently also $S_2O_3^{2-}$ [Reaction (5)]. In contrast to thiosulfate oxidation of organic matter, the oxidation involving SO_4^{2-} results only in water and CO_2. The by-product of both types of oxidation is sulfite SO_3^{2-} which, in the presence of elemental sulfur, could again yield thiosulfate. Elemental sulfur can originate from, for example, S–S linkages in immature kerogen (Rospondek et al., 1994), which agrees with results obtained by Zhang et al. (2007). All these reagents cannot be detected after the process. However, the oxidised residual organic matter or oil would be enriched in aromatics. We propose therefore the application of triphenyleno[1,12-*bcd*]thiophene and other pericyclic aromatic compounds like triphenylene (formed from *o*-terphenyl; see Marynowski et al., 2001), benzopyrenes, perylene, etc. as molecular markers for thermochemical sulfate reduction.

5. Conclusions

The modelled thermodynamic equilibrium composition of phenyldibenzothiophenes comes close to that obtained in laboratory maturation experiments and encountered in mature samples ($R_r \sim 1.2\%$). Such a mixture is composed of abundant 2- and 3-isomers, medium 4-isomer and very minor 1-PhDBT. One possible way for leading to the formation of thermodynamically controlled mixtures is likely to be a 1,2-phenyl shift catalysed by acid. Exclusively, when acid catalysed, the reaction has a low estimated activation energy [$\Delta E_{(aq)}$ ranging from 20.5 to 28.7 kcal/mol]. The range is consistent with geological data indicating a decrease in unstable isomer abundances associated with an increase in the stable isomers beginning at the onset of oil generation. In terms of the 1,2-phenyl shift, the energy barrier could be lower than that for the analogous 1,2-methyl shift for methyldibenzothiophene isomerisation, considering the differences in the distributions of both groups in geological samples. The cyclisation of 1-PhDBT to triphenyleno[1,12-*bcd*]thiophene is expected to proceed in nature only at advanced stages of diagenesis/catagenesis owing to the higher rate controlling energy barrier $\Delta E_{(aq)}$ in range 61–64 kcal/mol, depending on fluid properties, which is again promoted by acid catalysis and requires association with oxidation. The modelled energy barrier for dehydrocyclisation (oxidation) of 1-PhDBT to triphenyleno[1,12-*bcd*]thiophene with thiosulfate is about the energy range

for thermochemical sulfate reduction. We postulate the application of triphenyleno[1,12-*bcd*]thiophene and other pericyclic aromatic compounds (e.g. triphenylene, benzofluarantenes) as molecular markers for late diagenetic/catagenetic (epigenetic) oxidation, most likely related to the commonly observed thermochemical sulfate reduction.

Acknowledgements

The study was supported by a KBN (Polish Committee for Sciences) Grant PB0354/P04/2003/25 to M.R., and was partly financed by MNISW Grant N N307 2379 33 to L.M. and a Jagiellonian University DS and BW grants. Quantum chemical calculations were performed with a SGI 3700 workstation at ACK Cyfronet AGH (Grant Nos. MNiSW/SGI3700/PAN/137/2007 and MNiSW/SGI4700/UJ/075/2007). The authors thank the geologists from KGHM S.A., J. Kubiak, J. Jamróz, A. Witrykus and R. Reutt for logistic support in the mines and D. Clowes for improving the english. We acknowledge B.R.T. Simoneit for the sample of hydrothermal petroleum from the Guaymas Basin and R. Meyer zu Reckendorf for providing phenyldibenzothiophene standards. W. Wirski is acknowledged for donation of PC to M.R. Technical assistance by S. Kurkiewicz is gratefully acknowledged. The manuscript benefitted from constructive reviews by two anonymous reviewers.

Appendix A

Numbering of carbons in dibenzothiophene is shown in the following figure.

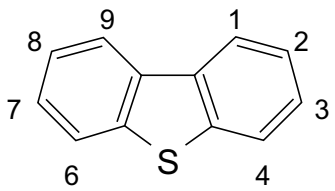

Appendix B

The most important transition state (TS) structures discussed in the text.

Structure of TS1:

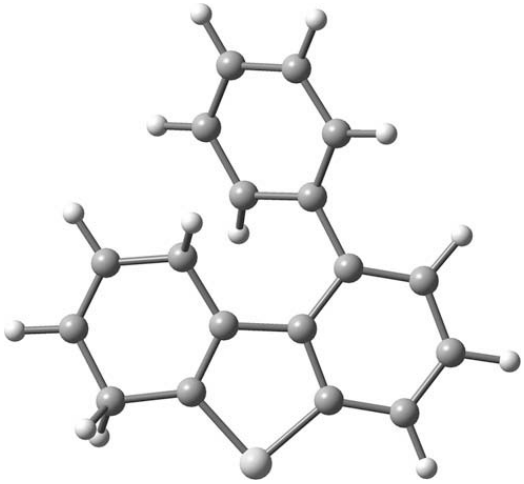

Structure of TS2:

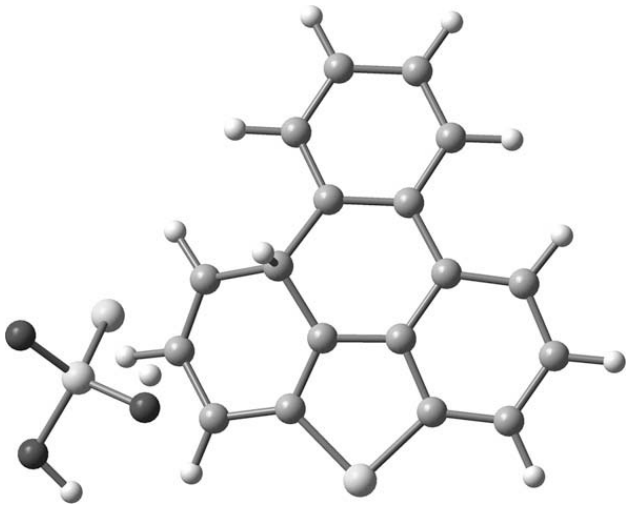

Structure of TS3:

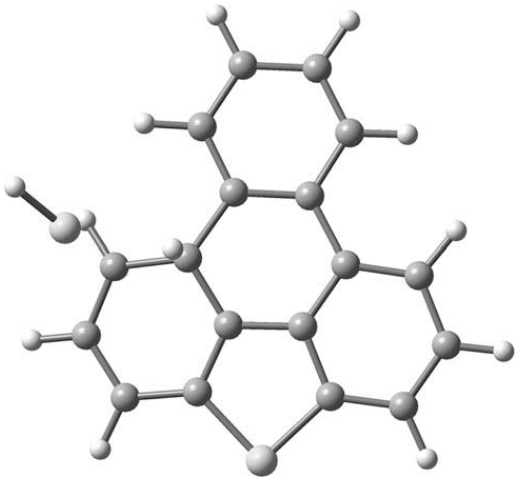

Structure of TS3_HS:

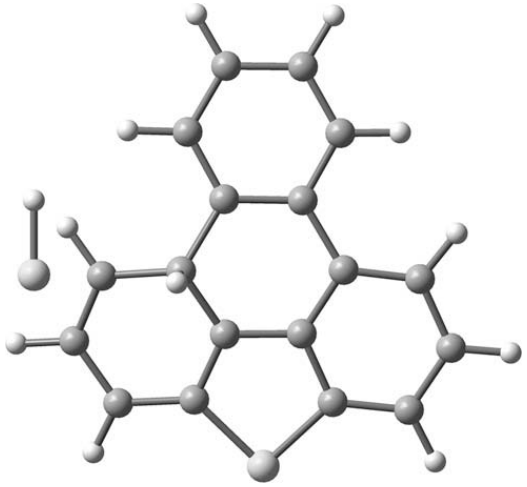

Structure of TS1–2:

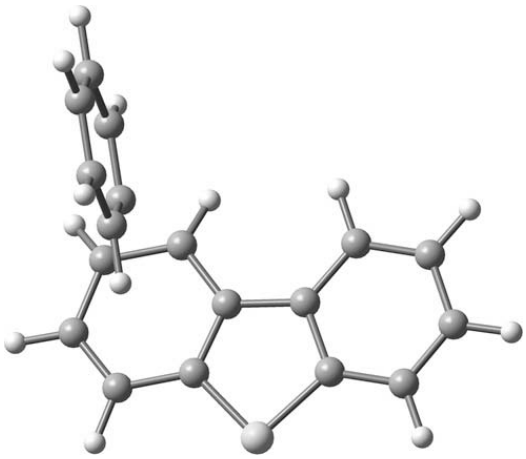

Associate Editor—**R. di Primio**

References

Akiya, N., Savage, P.E., 2002. Roles of water for chemical reactions in high-temperature water. Chemical Reviews 102, 2725–2750.

Bechtel, A., Sun, Y., Püttmann, W., Hoernes, S., Hoefs, J., 2001. Isotopic evidence for multi-stage base metal enrichment in the Kupferschiefer from the Sangerhausen Basin, Germany. Chemical Geology 176, 31–49.

Bechtel, A., Gartzer, R., Püttmann, W., Oszczepalski, S., 2002. Geochemical characteristics across the oxic/anoxic interface (Rote Fäule front) within the Kupferschiefer of the Lubin-Sieroszowice mining district (SW Poland). Chemical Geology 185, 9–31.

Becke, A.D., 1993. Density-functional thermochemistry. 3. The role of exact exchange. Journal of Chemical Physics 98, 5648–5652.

Budzinski, H., Garrigues, P., Radke, M., Connan, J., Oudin, J.-L., 1993. Thermodynamic calculations on alkylated phenanthrenes: geochemical applications to maturity and origin of hydrocarbons. Organic Geochemistry 20, 917–926.

Chakhmakhchev, A., Suzuki, M., Takayama, K., 1997. Distribution of alkylated dibenzothiophenes in petroleum as a tool for maturation assessments. Organic Geochemistry 26, 483–490.

Dartiguelongue, C., Behar, F., Budzinski, H., Scacchi, G., Marquaire, P.M., 2006. Thermal stability of dibenzothiophene in closed system pyrolysis: experimental study and kinetic modelling. Organic Geochemistry 37, 98–116.

Descostes, M., Vitorge, P., Beaucaire, C., 2004. Pyrite dissolution in acidic media. Geochimica et Cosmochimica Acta 68, 4559–4569.

Dewar, M.J.S., Zoebisch, E.G., Healy, E.F., 1985. AM1: a new general purpose quantum mechanical molecular model. Journal of the American Chemical Society 107, 3902–3909.

Ellis, G.S., Zhang, T., Ma, Q., Tang, Y., 2007. Kinetics and mechanisms of hydrocarbon oxidation by thermochemical sulfate reduction. In: Farrimond, P. et al. (Eds.), Book of Abstracts, 23th International Meeting on Organic Geochemistry, Torquay, England, pp. 299–300.

Frisch, M.J., Trucks, G.W., Schlegel, H.B., Scuseria, G.E., Robb, M.A., Cheeseman, J.R.T., Montgomery, J.A., Vreven, J.T., Kudin, K.N., Burant, J.C., Millam, J.M., Iyengar, S.S., Tomasi, J., Barone, V., Mannucci, B., Cossi, M., Scalmani, G., Rega, N., Petersson, G.A., Nakatsuji, H., Hada, M., Ehara, M., Toyota, K., Fukuda, F., Hasegawa, J., Ishida, M., Nakajima, T., Honda, Y., Kitao, O., Nakai, H., Klene, M., Li, X., Knox, J.E., Hratchian, H.P., Cross, J.B., Bakken, V., Adamo, C., Jramillo, J., Gomperts, R., Stratmann, R.E., Yazyev, O., Austin, A.J., Cammi, R., Pomelli, C., Ochterski, J.W., Ayala, P.Y., Morokuma, K., Voth, G.A., Salvador, P., Dannenberg, J.J., Zakrzewski, V.G., Dapprich, S., Daniels, A.D., Strain, M.C., Frakas, O., Malick, D.K., Rabuck, A.D., Raghavachari, K., Foresman, J.B., Ortiz, J.V., Cui, Q., Baboul, A.G., Clifford, S., Cislowski, J., Stefanov, B.B., Liu, G., Liashenko, A., Piskorz, P., Komaromi, I., Martin, R.L., Fox, D.J., Keith, T., Al-Laham, M.A., Peng, C.Y., Nanayakkara, A., Challacombe, M., Gill, P.M.W., Johnson, B., Chen, W., Wong, M.W., Gonzalez, C., Pople, J.A., 2004. Gaussian-94, Revision C.3, Gaussian, Inc., Pittsburgh, PA.

Goldhaber, M.B., Orr, W.L., 1995. Kinetic controls on thermochemical sulfate reduction as a source of sedimentary H2S. In: Vairavamurthy, M.A., Schoonen, M.A.A. (Eds.), Geochemical Transformations of Sedimentary Sulfur, ACS Symposium Series 612. American Chemical Society, Washington, D.C, pp. 412–425.

Graner, H.C., Warren, C.G., 1969. Unstable sulfur compounds and the origin of roll-type uranium deposits. Economic Geology 64, 160–171.

Janecky, D.R., Seyfried Jr., W.E., 1983. The solubility of magnesium-hydroxide–sulfate-hydrate in seawater at elevated temperatures and pressures. American Journal of Science 283, 831–860.

Jensen, F., 2001. Introduction to Computational Chemistry. Wiley, Chichester, UK.

Jørgensen, B.B., 1990. A thiosulfate shunt in the sulfur cycle of marine sediments. Science 249, 152–154.

Kagi, R.I., Alexander, R., Toh, E., 1990. Kinetics and mechanism of cyclization reaction of *ortho*-methylbiphenyls. In: Durand, B., Behar, F. (Eds.), Advances in Organic Geochemistry 1989 (Organic Geochemistry 16), 161–166.

Kawka, O.E., Simoneit, B.R.T., 1990. Polycyclic aromatic hydrocarbons in hydrothermal petroleums from the Guaymas Basin spreading centre. In: Simoneit, B.R.T. (Ed.), Organic Matter Alteration in Hydrothermal Systems – Petroleum Generation, Migration and Biogeochemistry. Applied Geochemistry 5, 17–27.

Killops, S.D., Massoud, M.S., 1992. Polycyclic aromatic hydrocarbons of pyrolytic origin in ancient sediments: evidence for Jurassic vegetation fires. Organic Geochemistry 18, 1–7.

Kotarba, M.J., Peryt, T.M., Kosakowski, P., Więcław, D., 2006. Organic geochemistry, depositional history and hydrocarbon generation modelling of the Upper Permian Kupferschiefer and Zechstein Limestone strata in south-west Poland. Marine and Petroleum Geology 23, 371–386.

Lee, C., Yang, W., Parr, R.G., 1988. Development of the Colle-Salvetti correlation-energy formula into a functional of the electron density. Physical Review B 37, 785–789.

Lewandowska, A., 1991. Minerals of the zone of altered Devonian dolomites from Dubie near Kraków (Southern Poland). Mineralogia Polonica 22, 29–40.

Lewandowska, A., 2000. Contact metamorphism induced by late Palaeozoic igneous activity in the Dębnik anticline. Polskie Towarzystwo Mineralogiczne – Prace Specjalne 17, 41–46.

Marynowski, L., Narkiewicz, M., Grelowski, C., 2000. Biomarkers as environmental indicators in a carbonate complex; examples from the Middle Devonian, the Holy Cross Mountains, Poland. Sedimentary Geology 137, 187–212.

Marynowski, L., Czechowski, F., Simoneit, B.R.T., 2001. Phenylnaphthalenes and polyphenyls in Palaeozoic source rocks of the Holy Cross Mountains, Poland. Organic Geochemistry 32, 69–85.

Marynowski, L., Rospondek, M., Meyer zu Reckendorf, R., Simoneit, B.R.T., 2002. Phenyldibenzofurans and phenyldibenzothiophenes in marine sedimentary rocks and hydrothermal petroleum. Organic Geochemistry 33, 701–714.

McCollom, T.M., Seewald, J.S., Simoneit, B.R.T., 2001. Reactivity of monocyclic aromatic compounds under hydrothermal conditions. Geochimica et Cosmochimica Acta 65, 455–468.

Meyer zu Reckendorf, R., 2000. Phenyl-substituted polycyclic aromatic compounds as intermediate products during pyrolytic reactions involving coal tars, pitches and related materials. Chromatographia 52, 67–76.

Miertus, S., Scrocco, E., Tomasi, J., 1981. Electrostatic interaction of a solute with a continuum. A direct utilizaion of ab initio molecular potentials for the prevision of solvent effects. Chemical Physics 55, 117–129.

Moore, D.M., Reynolds, R.C., 1997. X-ray Diffraction and the Identification and Analysis of Clay minerals. Oxford University Press, New York. pp. 378.

Nawrocki, J., Lewandowska, A., Fanning, M., 2007. Isotope and paleomagnetic ages of the Zalas rhyodacites (S Poland). Przegląd Geologiczny 55, 475–478.

Ohmoto, H., Lasaga, A.C., 1982. Kinetics of reactions between aqueous sulfates and sulfides in hydrothermal systems. Geochimica et Cosmochimica Acta 46, 1727–1745.

Oldenburg, T.B.P., Wilkes, H., Horsfield, B., van Duin, A.C.T., Stoddart, D., 2002. Xanthones – novel aromatic oxygen-containing compounds in crude oils. Organic Geochemistry 33, 595–609.

Oszczepalski, S., 1989. Kupferschiefer in Southwestern Poland: Sedimentary environments, metal zoning, and ore controls. In: Boyle, R.W., Brown, A.C., Jefferson, C.W, Jowett, E.C., Kirkham, R.W.

(Eds.), Sediment Hosted Stratiform Copper Deposits. Geological Association of Canada, Special Papers 36, pp. 571–600.
Otto, A., Simoneit, B.R.T., 1999. Chemosystematics and diagenesis of terpenoids in fossil conifer species and sediment from the Eocene Zeitz formation, Saxony, Germany. Geochimica et Cosmochimica Acta 65, 3505–3527.
Pitzer, K.S., 1983. Dielectric constant of water at very high temperature and pressure. Proceedings of the National Academy of Sciences of the United States of America 80, 4575–4576.
Püttmann, W., Villar, H., 1987. Occurrence and geochemical significance of 1,2,5,6-tetramethylnaphthalene. Geochimica et Cosmochimica Acta 51, 3023–3029.
Püttmann, W., Heppenheimer, H., Diedel, R., 1990. Accumulation of copper in the Permian Kupferschiefer: A result of post-depositional redox reactions. In: Durand, B., Tissot, B.P. (Eds.), Advances in Organic Geochemistry 1989 (Organic Geochemistry 16), 1145–1156.
Radke, M., Willsch, H., 1994. Extractable alkyldibenzothiophenes in Posidonia Shale (Toarcian) source rocks: relationship of yields to petroleum formation and expulsion. Geochimica et Cosmochimica Acta 58, 5223–5244.
Radke, M., Welte, D.H., Willsch, H., 1982. Geochemical study on a well in the Western Canada Basin: relation of the aromatic distribution pattern to maturity of organic matter. Geochimica et Cosmochimica Acta 46, 1–10.
Radke, M., Welte, D.H., Willsch, H., 1986. Maturity parameters based on aromatic hydrocarbons: influence of the organic matter type. In: Leythaeuser, D., Rullkötter, J. (Eds.), Advances in Organic Geochemistry 1985 (Organic Geochemistry 10), 51–63.
Radke, M., Vriend, S.P., Ramanampisao, L.R., 2000. Alkyldibenzofurans in terrestrial rocks: influence of organic facies and maturation. Geochimica et Cosmochimica Acta 64, 275–286.
Rospondek, M.J., Fijałkowska, A., Lewandowska, A., 1993. The origin of organic matter in Lower Silesian copper-bearing shales. Rocznik Polskiego Towarzystwa Geologicznego 63, 85–99.
Rospondek, M.J., de Leeuw, J.W., Baas, M., van Bergen, P.F., Leereveld, H., 1994. The role of organically bound sulphur in stratiform ore sulphide deposits. Organic Geochemistry 21, 1181–1191.
Rospondek, M.J., Marynowski, L., 2004. Phenyl-polyaromatic compounds and terphenyls in the Polish Carpathian sedimentary rocks. Polskie Towarzystwo Mineralogiczne, Prace Specjalne 24, 341–344.
Rospondek, M.J., Marynowski, L., Góra, M., 2007. Novel arylated polyaromatic thiophenes: phenylnaphtho[*b*]thiophenes and naphthylbenzo[*b*]thiophenes as markers of organic matter diagenesis buffered by oxidising solutions. Organic Geochemistry 38, 1729–1756.
Sawłowicz, Z., 1993. Organic matter and its significance for the genesis of the copper-bearing shales (Kupferschiefer) from the Fore-Sudetic Monocline (Poland). In: Parnell, J., Kucha, H., Landais, P. (Eds.), Bitumens in Ore Deposits. Springer, Berlin, pp. 431–446.
Schmidt, M.W., Baldridge, K.K., Boatz, J.A., Elbert, S.T., Gordon, M.S., Jensen, J.H., Koseki, S., Matsunaga, N., Nguyen, K.A., Su, S.J., Windus, T.L., Dupuis, M., Montgomery, J.A., 1993. General atomic and molecular electronic structure system. Journal of Computational Chemistry 14, 1347–1363.
Seewald, J.S., 1997. Mineral redox buffers and the stability of organic compounds under hydrothermal conditions. In: Materials Research Society Symposium Proceedings, vol. 432, pp. 317–331.
Seewald, J.S., 2003. Organic–inorganic interactions in petroleum-producing sedimentary basins. Nature 426, 327–333.
Seewald, J.S., Eglinton, L.B., Ong, Y.-L., 2000. Organic–inorganic interactions during vitrinite maturation. Geochimica et Cosmochimica Acta 64, 1577–1591.
Simoneit, B.R.T., 1993. Aqueous high temperature and high pressure organic geochemistry of hydrothermal vent systems. Geochimica et Cosmochimica Acta 57, 3231–3243.
Spagnolo, P., Testaferri, L., Tiecco, M., Martelli, G., 1972. The reactivity of thieno[3,2-*b*]thiophene and thieno[2,3-*b*]thiophene with phenyl radicals. Journal of the Chemical Society, Perkin Transactions I, 93–96.
Środoń, J., Kotarba, M., Biroň, A., Such, P., Clauer, N., Wójtowicz, A., 2006. Diagenetic history of the Podhale-Orava Basin and the underlying Tatra sedimentary structural units (Western Carpathians): evidence from XRD and K–Ar of illite-smectite. Clay Minerals 41, 751–774.
Strachan, M.G., Alexander, R., Kagi, R.I., 1988. Trimethylnaphthalenes in crude oils and sediments: effects of source and maturity. Geochimica et Cosmochimica Acta 52, 1255–1264.
Sun, Y., Püttmann, W., Speczik, S., 1995. Differences in the depositional environment of basal Zechstein in southwest Poland: implications for base metal mineralization. Organic Geochemistry 23, 819–835.
Toland, W.G., 1960. Oxidation of organic compounds in aqueous sulfate. Journal of the American Chemical Society 82, 1911–1916.
van Aarssen, B.G.K., Bastow, T.P., Alexander, R. Kagi, R.I., 2001. Identification of *n*-alkyl dibenzothiophenes in sedimentary organic matter. In: Abstracts 20th International Meeting on Organic Geochemistry, Nancy, pp. 301.
van Duin, A.C.T., Baas, J.M.A., de Graaf, W., de Leeuw, J.W., Bastow, T.P., Alexander, R., 1997. Comparison of calculated equilibrium mixtures of alkylnaphthalenes and alkylphenanthrenes with experimental data; the importance of entropy calculations. Organic Geochemistry 26, 275–280.
Wei, Z., Moldowan, M.J., Dahl, J., Goldstein, T.P., Jarvie, D.M., 2006. The catalytic effects of minerals on the formation of diamondoids from kerogen macromolecules. Organic Geochemistry 37, 1421–1436.
Xu, Y., Schoonen, M.A.A., Nordstrom, D.K., Cunningham, K.M., Ball, J.W., 1998. Sulfur geochemistry of hydrothermal waters in Yellowstone National Park: I. The origin of thiosulfate in hot spring waters. Geochimica et Cosmochimica Acta 62, 3729–3743.
Zhang, T., Ellis, G.S., Wang, K., Walters, C.C., Kelemen, S.R., Gillaizeau, B., Tang, Y., 2007. Effect of hydrocarbon type on thermochemical sulfate reduction. Organic Geochemistry 38, 897–910.
Zhang, T., Ellis, G.S., Walters, C.C., Kelemen, S.R., Wang, K., Tang, Y., 2008. Geochemical signatures of thermochemical sulfate reduction in controlled hydrous pyrolysis experiments. Organic Geochemistry 39, 308–328.